

Dynamic response analysis of induction motor drive influenced by controller design methods

Panuwat Kaewma, Nattapong Pothi, Chawasak Rakpenthai

Department of Electrical Engineering, School of Engineering, University of Phayao, Phayao, Thailand

Article Info

Article history:

Received Feb 22, 2024

Revised Nov 10, 2024

Accepted Nov 28, 2024

Keywords:

Controller design

Dynamic response

Field-oriented control

Induction motor drives

Tracking accuracy

ABSTRACT

This paper proposes a comparison study focusing on the dynamic response and tracking accuracy for the induction motor drive system influenced by the controller design methods. Pole-zero cancellation (PZC) and pole placement (PP) methods are commonly used to define the controller gains for motor drive systems, and both methods are verified in this paper. The bandwidth of controllers for both methods is set equally based on the field-oriented control strategy, which consists of current and speed control loops. Furthermore, the test conditions are defined to examine the drive system performance, i.e., i) load torque rapidly changes with the maintained speed and ii) speed changes in no-load and with-load torque conditions to validate the current and speed control loops, respectively. The validation of the drive system performance influenced by the controller design methods is demonstrated by simulation results.

This is an open access article under the [CC BY-SA](https://creativecommons.org/licenses/by-sa/4.0/) license.



Corresponding Author:

Nattapong Pothi

Department of Electrical Engineering, School of Engineering, University of Phayao

19 Moo.2, Meaka, Muang Phayao, Phayao 56000, Thailand

Email: nattapong.po@up.ac.th

1. INTRODUCTION

Induction motors (IMs) have gained widespread acceptance and become the primary power source in numerous sectors, such as manufacturing, agriculture, and household applications. It is due to the merits of such motors, including robustness, reliability, simplicity, cost-effectiveness, low maintenance requirements, and high efficiency [1], [2]. In addition, for some specific applications, e.g., pumps, compressors, elevators, electric vehicles, and military technology, high-precision control is usually required for variable speed drives (VSDs) and can also enhance the drive system performance [3], [4]. Because the field-oriented control (FOC) method, which can also be called a vector control method, offers a fast dynamic response, low torque ripple, and good tracking accuracy, it would be the best alternative for high-precision control of IM drives [5], [6].

Based on the principle of the FOC method, the rotor flux-linkage can be independently controlled through the d -axis current, while the q -axis current is used to produce the induced torque corresponding to the load-torque requirement [7]. Consequently, the rotor flux-linkage and torque can be controlled separately. Since there are three feedback control loops for the speed control of the FOC method, in which the speed and q -axis current control loops are cascaded, an inappropriate design of bandwidths and controller gains can influence the drive performance [8]. Therefore, numerous approaches have been proposed to enhance the tracking accuracy and dynamic response of the controllers. Fuzzy logic is applied instead of the speed controller for the IM drive [9], [10], and an artificial neural network is also presented in [11] to compensate for the current controller gains, resulting in a robust IM drive system. Similarly, a model predictive control (MPC) is utilized to calculate stator reference voltages to generate switching signals for the voltage source inverter (VSI) instead of using current controllers [12]. Complex vector controller is presented for reducing the effects of cross-

coupling and providing robustness to parameter variations [13]. Kuperman [14], explained a resonant current controller is considered for synchronizing the frequency response to handle harmonics that disturb the drive system, and it is also improved for simple implementation in [15]. Besides, the dynamic response of the speed controller is improved in terms of overshoot presented in [16] and [17] by using the IP controller, and a robust drive system, e.g., inertia variation, parameters variation, and load disturbances, can be achieved by considering a two-degree-of-freedom controller configuration in the speed control loop [18], [19].

Although the several methods offer good performance, the computational burden and complexity of usage remain significant concerns. Nevertheless, since the proportional and integral (PI) controller can offer sufficient dynamic response, good tracking performance, a simple structure, and ease of implementation, it is still widely considered in motor drive systems [8]. The PI controller gains can usually be determined by using either the pole-zero cancellation (PZC) method [20]-[22] or the pole placement (PP) method [23], [24]. Even though the PZC method is simple, the closed-loop transfer function of the tracking system is reduced to first order. In contrast, for the PP method, the characteristic equation of the closed-loop transfer function is mainly utilized. Both the damping ratio and natural frequency have to be defined properly [25], which can directly affect the drive system's performance, resulting in more complexity than the PZC method. Consequently, the dynamic response and tracking accuracy of both controller design methods should be realized.

This article presents a comparative analysis of the IM drive system performance, regarding dynamic response and tracking accuracy, influenced by the controller design between the PZC and PP methods. The bandwidth of controllers for both methods is set equally based on the FOC strategy. The overall performance comparison of both controller design methods is verified by simulation results.

2. INDUCTION MOTOR AND FIELD-ORIENTED CONTROL

2.1. Mathematical model

The d -axis and q -axis stator voltages and induced torque that have been arranged in the synchronous reference frame are given in (1)-(3), respectively.

$$v_{ds} = R_s' i_{ds} + \sigma L_s \frac{di_{ds}}{dt} - \omega_e \sigma L_s i_{qs} - R_r \frac{L_m}{L_r} \psi_{dr} \quad (1)$$

$$v_{qs} = R_s' i_{qs} + \sigma L_s \frac{di_{qs}}{dt} + \omega_e \sigma L_s i_{ds} + \omega_{sl} \frac{L_m}{L_r} \psi_{dr} \quad (2)$$

$$T_e = \frac{3}{2} \frac{L_m}{L_r} P (\psi_{dr} i_{qs} - \psi_{qr} i_{ds}) \quad (3)$$

Where $R_s' = R_s + R_r(L_m/L_r)^2$ denotes stator transient resistance, R_r is rotor winding resistance, L_m is mutual inductance, L_s, L_r are stator and rotor inductances, respectively, ω_e, ω_{sl} are electric angular and slip velocities, P is pole pairs, ψ_{dr}, ψ_{qr} are rotor flux-linkage of d - and q -axes, respectively, and $\sigma = (1 - (L_m^2/L_s L_r))$ is leakage coefficient.

The induced torque can also be represented by considering the mechanical elements, as given in (4).

$$T_e = J \frac{d\omega_m}{dt} + B \omega_m + T_L \quad (4)$$

Where J, B denote moment of inertia and friction coefficient, respectively, ω_m is mechanical angular velocity, and T_L is the load-torque.

2.2. Field oriented control of induction motors

The FOC strategy, as shown in Figure 1, is the vector control method that have been widely applied in induction motor drive systems due to low-torque ripple and low acoustic noise. This approach allows both rotor flux-linkage and torque to be controlled separately through the control of d -axis and q -axis currents, respectively [7]. Indeed, the d -axis reference current is defined by (5), while the q -axis reference current is determined in accordance with the speed control loop [18]. The slip angular velocity and electrical angular position, which are utilized in the FOC system, can be calculated by (6) and (7), respectively.

$$i_{ds}^* = \frac{\psi_{dr}}{L_m} \quad (5)$$

$$\omega_{sl} = \frac{R_r i_{qs}}{L_r i_{ds}} \quad (6)$$

$$\theta_e = \int \omega_e dt = \int (\omega_{sl} + \omega_m) dt \quad (7)$$

Where ω_{sl} is slip angular velocity in rad/s, and * indicates the reference value.

The closed-loop diagrams with the PI controller of both d -axis current and speed controls are expressed in Figures 2(a) and 2(b), respectively. Those can also be arranged into the closed-loop transfer function that is utilized to design the controller gains of d - q axis currents and speed control loops, as given in (8)-(10) [20].

$$\frac{i_{ds}(s)}{i_{ds}^*(s)} = \frac{sk_{pc,d} + k_{ic,d}}{s^2(\sigma L_s) + s(R'_s + k_{pc,d}) + k_{ic,d}} \quad (8)$$

$$\frac{i_{qs}(s)}{i_{qs}^*(s)} = \frac{sk_{pc,q} + k_{ic,q}}{s^2(\sigma L_s) + s(R'_s + k_{pc,q}) + k_{ic,q}} \quad (9)$$

$$\frac{\omega_m(s)}{\omega_m^*(s)} = \frac{(sk_{ps} + k_{is})k_T}{s^2 J + s(B + k_{ps}k_T) + k_{is}k_T} \quad (10)$$

Where s denotes a complex frequency domain in Laplace transform, $k_{pc,d}$, $k_{ic,d}$, $k_{pc,q}$, $k_{ic,q}$ are proportional and integral gains of d -axis and q -axis current controllers, respectively, k_{ps} , k_{is} are proportional and integral gains of speed controller, and $k_T = 1.5 (L_m/L_r) \cdot P \psi_{dr}$.

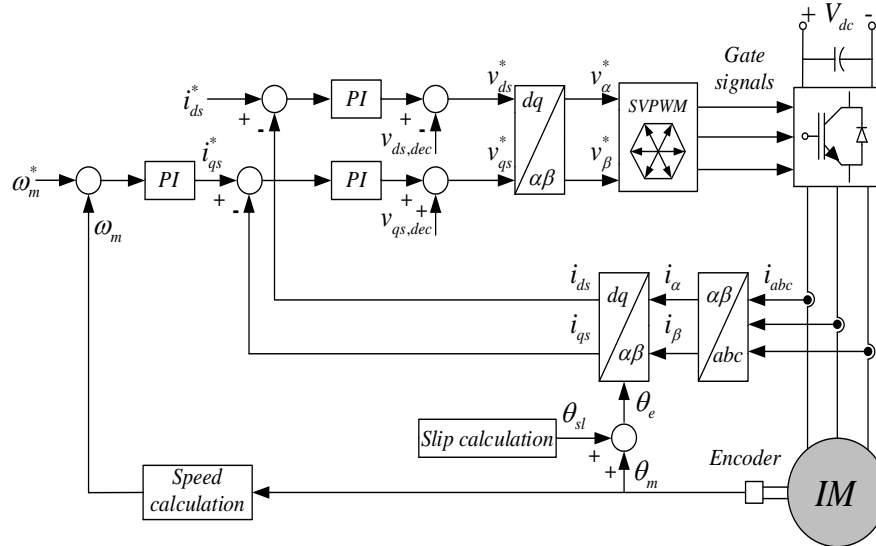


Figure 1. Control diagram based on the FOC method for three-phase induction motors

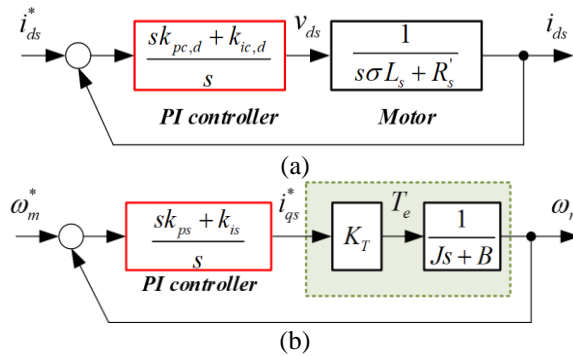


Figure 2. Current and speed controls with the PI controller: (a) d -axis current and (b) speed

3. CONTROLLER DESIGN METHODS

3.1. Pole-zero cancellation method

The pole-zero cancellation (PZC) method is generally employed to design the PI controller gains in both DC and AC drive systems due to its simplicity, where only machine parameters and bandwidth selection are required. For the current control loop, as illustrated in Figure 2(a), the zero of the PI controller ($-k_{ic,d}/k_{pc,d}$) is set to cancel the dominant pole of the motor ($-R'_s/\sigma L_s$), leaving only the zero at the origin. Accordingly, the closed-loop transfer function of the current control will be reduced to first-order [20], [21]. The bandwidth of the current control loop is normally defined as at least 10 times lower than the switching frequency (f_s) [7]. The current controller gains of both d -axis and q -axis PI controllers can simply be designed by (11) and (12), respectively.

$$k_{pc,d} = \sigma L_s \omega_{bc}, \quad k_{ic,d} = R'_s \omega_{bc} \quad (11)$$

$$k_{pc,q} = \sigma L_s \omega_{bc}, \quad k_{ic,q} = R'_s \omega_{bc} \quad (12)$$

Where ω_{bc} is the bandwidth of current control loop, $\omega_{bc} = 2\pi f_s/10$.

For the speed control loop, as expressed in Figure 2(b), the closed-loop transfer function consists of the mechanical components mentioned in (4). The controller gains can be determined similarly to the case of the current control loop, which the zero of the PI controller ($-k_{is}/k_{ps}$) is designed to cancel the dominant pole of the speed control loop ($-B/J$). The torque constant (k_T) is considered to transform the torque quantity into the q -axis reference current to support the current control loop based on the FOC strategy, as illustrated in Figure 1. The PI controller gains for the speed control loop can be designed by (13).

$$k_{ps} = \frac{J \omega_{bs}}{k_T}, \quad k_{is} = \frac{B \omega_{bs}}{k_T} \quad (13)$$

Where k_{ps} , k_{is} are proportional and integral gains of speed controller, respectively, and ω_{bs} is the bandwidth of speed control loop, $\omega_{bs} = \omega_{bc}/10$.

3.2. Pole placement method

The pole placement (PP) method is based on an analysis of the closed-loop transfer function of the IM, as mentioned in (8)-(10) for the d - q axis currents and speed control loops, respectively. In this method, the denominator of the closed-loop transfer function expressed in the s -domain, which has been called the characteristic equation, is arranged into the second-order polynomial function that is commonly considered in the control system. For the d -axis current control loop, the characteristic equation can be arranged and compared to the control function that consists of damping ratio (ξ) and natural frequency (ω_n), as shown in (14). Definitely, it can be considered identically for the q -axis current control loop. In order to achieve high performance in the drive system, the damping ratio and the natural frequency should be defined appropriately because they can directly affect the dynamic response and steady-state performance of the controller.

$$s^2 + s \left(\frac{R'_s + k_{pc,d}}{\sigma L_s} \right) + \frac{k_{ic,d}}{\sigma L_s} \Rightarrow s^2 + 2\xi \omega_n s + \omega_n^2 \quad (14)$$

The natural frequency can be presented in a related equation of the bandwidth and damping ratio, as given by (15) [22], [23]. The bandwidth is simply defined as a function of the switching frequency, while the damping ratio can be set at 0.707 ($\xi = 0.707$), which is the optimal point of the second-order polynomial function in the control system [23], [24]. Indeed, it can be considered similarly in the case of the speed control loop.

$$\omega_n = \frac{\omega_{bc}}{\sqrt{1 - 2\xi^2 + \sqrt{2 - 4\xi^2 + 4\xi^4}}} \quad (15)$$

By considering the characteristic equation expressed in (14), the current controller gains of both the d - and q -axes can be designed as given in (16) and (17), respectively.

$$k_{pc,d} = \sigma L_s 2\xi \omega_n - R'_s, \quad k_{ic,d} = \sigma L_s \omega_n^2 \quad (16)$$

$$k_{pc,q} = \sigma L_s 2\xi \omega_n - R'_s, \quad k_{ic,q} = \sigma L_s \omega_n^2 \quad (17)$$

For the speed control loop, the closed-loop transfer function is utilized, as aforementioned in (10), in which the moment of inertia and friction coefficient are considered. The denominator of the speed transfer function is similarly arranged to be the second-order polynomial function, as in the case of the current control loop indicated in (14). Hence, the PI controller gains based on the PP method of the speed control loop can be determined as given by (18).

$$k_{ps} = \frac{(2\xi\omega_n J) - B}{k_T}, \quad k_{is} = \frac{\omega_n^2 J}{k_T} \quad (18)$$

It is noted that the saturation of integration in both current and speed control loops based on the PP method might happen due to the high integral gain, which is proportional to the squared natural frequency, as mentioned in (16)-(18). Therefore, the anti-windup is crucially required to avoid the over-integration in the controller [25], but it might not be required in the PZC method. However, the closed-loop transfer function based on the PZC method is reduced to the first-order, which might affect the drive system's performance.

4. SIMULATION RESULTS VERIFICATION

A squirrel cage type three-phase induction motor 4.3 kW is considered to demonstrate the dynamic performance of both current and speed controllers caused by the design methods. The motor parameters are indicated in Table 1. The d -axis current reference is set at 6.3 A, corresponding to the rotor flux requirement of the motor. The current and speed controller gains of both controller design methods are given in Table 2. The switching frequency is set at 10 kHz, which is used to define the bandwidth and natural frequency, while the damping ratio is set at the optimal point ($\xi = 0.707$) for both current and speed control loops. The FOC strategy is used in the drive system implemented by the MATLAB/Simulink program. The voltage source inverter (VSI) is triggered based on the space-vector pulse width modulation (SVPWM) switching technique. Both controller design methods, i.e., PZC and PP methods, are compared and validated in terms of dynamic response performance and tracking accuracy.

Table 1. Motor parameters

Parameters	Symbols	Values
DC-link voltage	V_{dc}	600 V
Base speed	ω_b	1,450 rpm
Rated current	I_m	12.0 A
d -axis reference current	i_{ds}^*	6.3 A
Armature winding resistance	R_s	0.711 Ω
Rotor winding resistance	R_r	0.441 Ω
Leakage inductance of stator	L_{ls}	3.209 mH
Leakage inductance of rotor	L_{lr}	4.594 mH
Mutual inductance	L_m	69.78 mH
d -axis rotor flux	ψ_{dr}	0.4449 Wb
Moment of inertia	J	0.0138 kg·m ²
Friction coefficient	B	0.000503 Nm·s
Number of pole pairs	P	2
Leakage coefficient	σ	0.1030187

Table 2. PI controller gains setting

Controllers	PZC method	PP method
f_s	10 kHz	
ω_{bc}	6283.185 (rad/s)	
ω_{bs}	628.318 (rad/s)	
$k_{pc,db} \ k_{pc,q}$	47.244	65.694
$k_{ic,db} \ k_{ic,q}$	6906.5	296760
k_{ps}	8.6708	12.2582
k_{is}	0.3160	5446.4

Figure 3 shows the torque response compared between the PZC and PP methods. The load torque is set as a unit step, which rapidly changes from no-load (0 Nm) to 5.0 Nm at 0.2 s, while the motor speed is maintained at 500 rpm to verify the current control loop performance. The results show that the PZC method provides a percent overshoot (%OS) of around 26%, as illustrated in Figure 3(a), lower than the PP method, which is approximately 32%, as shown in Figure 3(b). It also corresponds to the result of the q -axis current following the principle of vector control, as shown in Figure 4, in which the overshoots of the q -axis current

of the PZC and PP methods are around 30% and 36.2%, respectively. However, the dynamic response of the torque and q -axis current based on the PP method is faster than the PZC method. The rise time (t_r) and settling time (t_s) of the q -axis current based on the PZC method are around 0.331 ms and 1.621 ms, respectively, while those results of the PP method are about 0.214 ms and 1.191 ms, respectively. Figure 5 shows the tracking d -axis current of both controller design methods. The rotor flux can achieve the setting value corresponding to good tracking of the flux-generated d -axis current. Furthermore, the PP method can also provide a better tracking accuracy of the machine speed than the PZC method, as specified in Figure 6. By maintaining the reference speed at 500 rpm operating with the load torque change conditions as abovementioned, the steady-state error (e_{ss}) of the machine speed based on the PZC method is approximately 0.2132%, while it is 0.0001% for the PP method, which is nearly zero. It should be noted that, for the current control loop verifications, although the PZC method can provide a low percent overshoot compared to the PP method, when the load torque suddenly changes, the PP method exhibits the merit of fast dynamic response and good tracking accuracy that can be observed from the steady-state error.

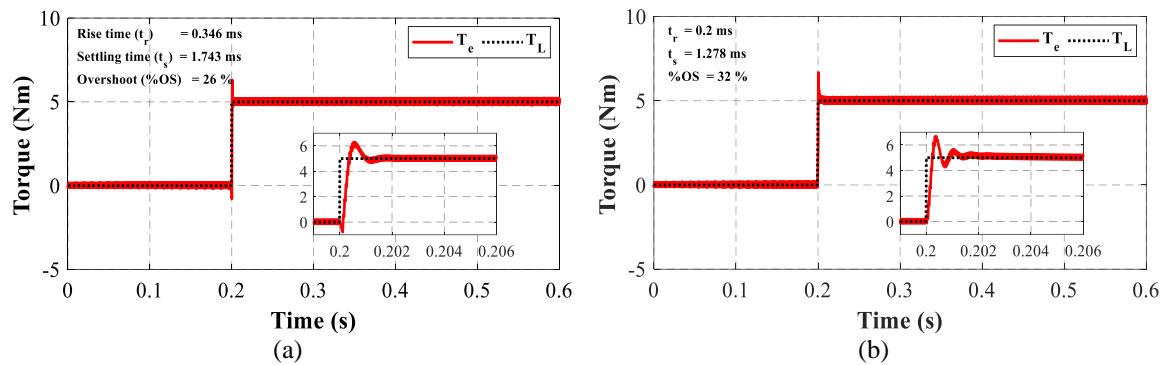


Figure 3. Torque response with a maintained speed of 500 rpm: (a) PZC and (b) PP

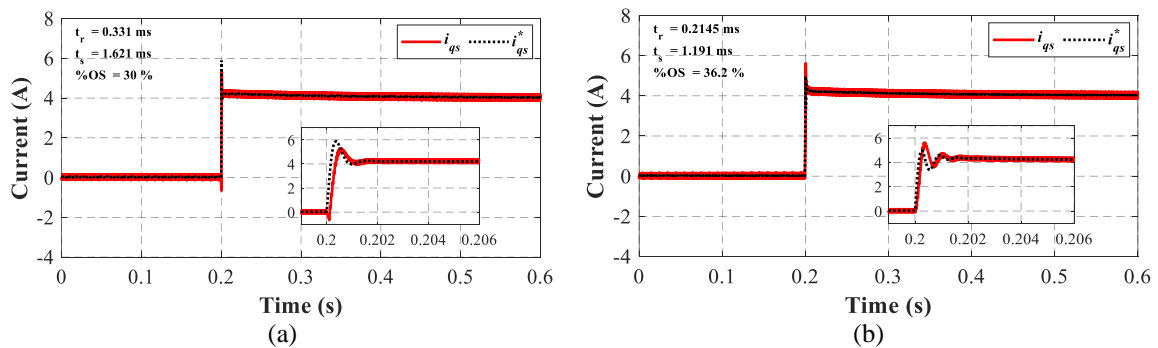


Figure 4. q -axis current response with a maintained speed of 500 rpm: (a) PZC and (b) PP

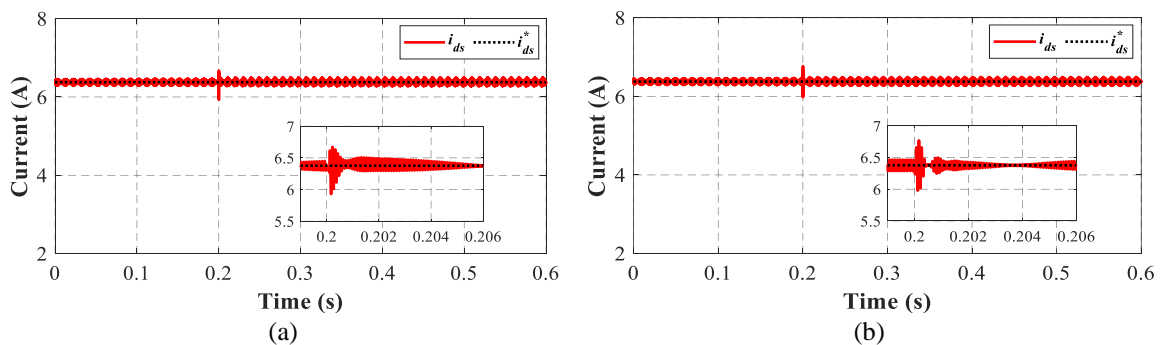


Figure 5. d -axis current response with a maintained speed of 500 rpm: (a) PZC and (b) PP

Likewise, for the speed control loop verifications, the reference speed is initially defined at 500 rpm and suddenly changes to 1,000 rpm at 0.2 s in both no-load and with-load torque conditions, as illustrated in Figures 7 and 8, respectively. For the no-load condition, the steady-state errors of the PZC method are around 0.068% with the speed at 500 rpm and 0.05% at 1,000 rpm, as indicated in Figure 7(a). Meanwhile, based on the PP method, the steady-state errors for the speed at 500 rpm and 1,000 rpm are almost zero, as shown in Figure 7(b). Because the controller bandwidth of both methods is equally defined, the dynamic responses of the machine speeds are also the same. For the with-load torque condition, the PP method can also provide excellent tracking accuracy of the speed control loop rather than the PZC method in which corresponds to the results in the case of the no-load condition, as shown in Figure 8.

Although the PZC method is quite simple to define the controller gains where only inductance and resistance of stator winding are required, the tracking accuracy of the speed control is still the main weakness point. The results show that the PP method can provide an outstanding dynamic response and better tracking accuracy performance than that of the PZC method in all verified conditions.

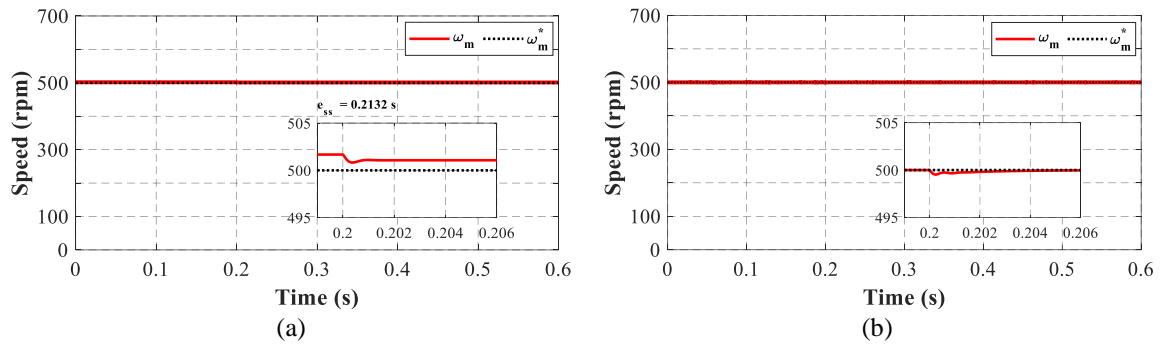


Figure 6. Speed response with a maintained speed at 500 rpm: (a) PZC and (b) PP

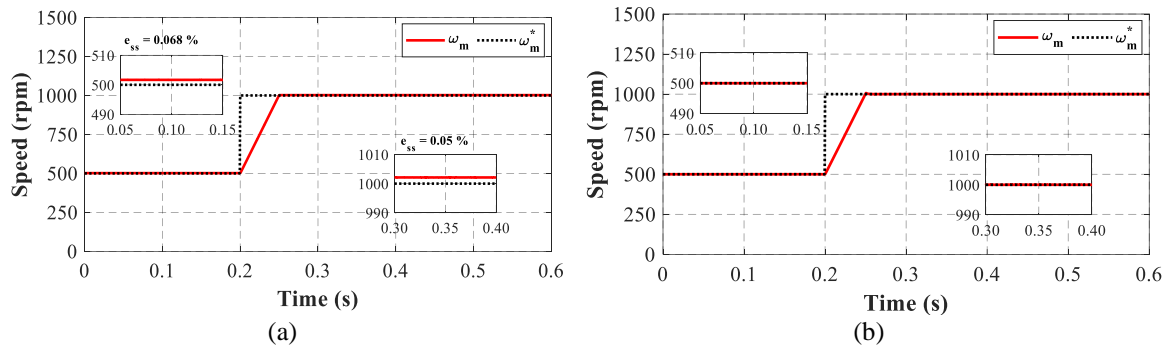


Figure 7. Speed response with no-load conditions ($T_L = 0$ Nm.): (a) PZC and (b) PP

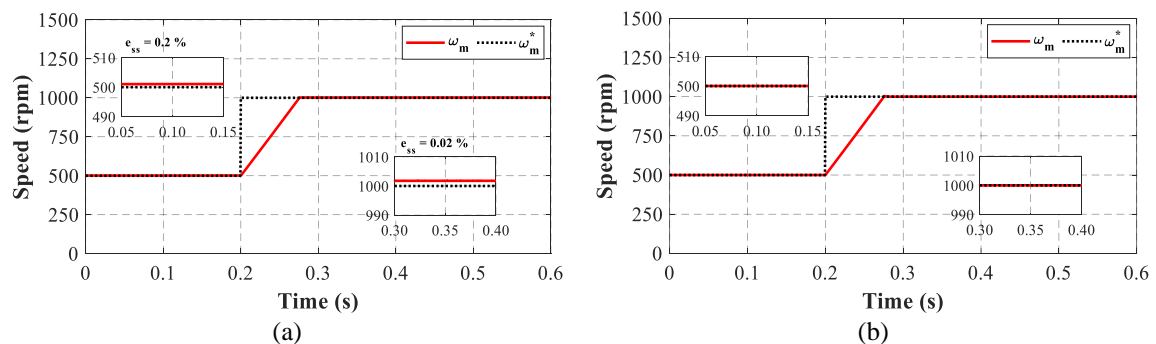


Figure 8. Speed response with-load torque condition ($T_L = 5.0$ Nm.): (a) PZC and (b) PP

5. CONCLUSION

Pole-zero cancellation (PZC) and pole placement (PP) methods, which both are commonly used to define the controller gains for motor drive systems based on field-oriented control (FOC) strategy, have been compared in terms of dynamic response and tracking accuracy performance in this paper. The test conditions, including: i) The load torque rapidly changing with the maintained speed and ii) The speed changing in no-load and with-load torque conditions, are considered to validate the controller performance. The results show that the PP method exhibits a faster response than the PZC method. When the load torque changes, the rise time and settling time of the q -axis current based on the PP method are about 0.214 ms and 1.191 ms, respectively, while in the case of the PZC method, they are 0.331 ms and 1.621 ms, respectively. It also corresponds to the result of the torque response. Furthermore, the PP method can provide better tracking accuracy than the PZC method in all verified conditions.





REFERENCES

- [1] K. Indriawati, F. P. Wijaya, and C. Mufit, "Implementation of disturbance observer for sensorless speed estimation in induction motor," *International Journal of Power Electronics and Drive Systems*, vol. 13, no. 2, pp. 724–732, 2022, doi: 10.11591/ijpeds.v13.i2.pp724-732.
- [2] B. Wang, J. Zhang, Y. Yu, X. Zhang, and D. Xu, "Unified complex vector field-weakening control for induction motor high-speed drives," *IEEE Transactions on Power Electronics*, vol. 36, no. 6, pp. 7000–7011, 2021, doi: 10.1109/TPEL.2020.3034246.
- [3] H. Bachiri, B. Gasbaoui, A. Ghezouani, and N. Nair, "Improved direct torque control strategy performances of electric vehicles induction motor," *International Journal of Power Electronics and Drive Systems*, vol. 13, no. 2, pp. 716–723, 2022, doi: 10.11591/ijpeds.v13.i2.pp716-723.
- [4] H. Gashtil, V. Pickert, D. J. Atkinson, M. Dahidah, and D. Giaouris, "Improved voltage boundary with model-based control algorithm for increased torque in the field weakening region of induction machines," *IEEE Transactions on Transportation Electrification*, vol. 7, no. 3, pp. 1600–1614, 2021, doi: 10.1109/TTE.2020.3048306.
- [5] C. Jung, C. R. C. Torrico, and E. Giovani Carati, "Adaptive loss model control for robustness and efficiency improvement of induction motor drives," *IEEE Transactions on Industrial Electronics*, vol. 69, no. 11, pp. 10893–10903, 2022, doi: 10.1109/TIE.2021.3125648.
- [6] S. Adigintla and M. V. Aware, "Robust fractional order speed controllers for induction motor under parameter variations and low speed operating regions," *IEEE Transactions on Circuits and Systems II: Express Briefs*, vol. 70, no. 3, pp. 1119–1123, 2023, doi: 10.1109/TCSII.2022.3220526.
- [7] S. M. Yang and K. W. Lin, "Automatic control loop tuning for permanent-magnet ac servo motor drives," *IEEE Transactions on Industrial Electronics*, vol. 63, no. 3, pp. 1499–1506, 2016, doi: 10.1109/TIE.2015.2495300.
- [8] A. T. Nguyen, M. S. Rafiq, H. H. Choi, and J. W. Jung, "A model reference adaptive control based speed controller for a surface-mounted permanent magnet synchronous motor drive," *IEEE Transactions on Industrial Electronics*, vol. 65, no. 12, pp. 9399–9409, 2018, doi: 10.1109/TIE.2018.2826480.
- [9] A. J. Ali, Z. K. Farej, and N. S. Sultan, "Performance evaluation of a hybrid fuzzy logic controller based on genetic algorithm for three phase induction motor drive," *International Journal of Power Electronics and Drive Systems*, vol. 10, no. 1, pp. 117–127, 2019, doi: 10.11591/ijpeds.v10.i1.pp117-127.
- [10] A. Sivakumar, M. Thiagarajan, and K. Kanagarathinam, "Mitigation of supply current harmonics in fuzzy-logic based 3-phase induction motor," *International Journal of Power Electronics and Drive Systems*, vol. 14, no. 1, pp. 266–274, 2023, doi: 10.11591/ijpeds.v14.i1.pp266-274.
- [11] X. Fu and S. Li, "A novel neural network vector control technique for induction motor drive," *IEEE Transactions on Energy Conversion*, vol. 30, no. 4, pp. 1428–1437, 2015, doi: 10.1109/TEC.2015.2436914.
- [12] T. B. Dos Santos, I. Olini, R. Figueiredo, D. Albieiro, A. Pelizari, and A. J. Sguarezi Filho, "Robust finite control set model predictive current control for induction motor using deadbeat approach in stationary frame," *IEEE Access*, vol. 11, pp. 13067–13078, 2023, doi: 10.1109/ACCESS.2022.3223385.
- [13] L. Wu et al., "Design of complex vector controller for high-power induction machine drive," *IEEE Transactions on Transportation Electrification*, vol. 10, no. 1, pp. 1816–1826, 2024, doi: 10.1109/TTE.2023.3265044.
- [14] A. Kuperman, "Proportional-resonant current controllers design based on desired transient performance," *IEEE Transactions on Power Electronics*, vol. 30, no. 10, pp. 5341–5345, 2015, doi: 10.1109/TPEL.2015.2408053.
- [15] M. Tian, B. Wang, Y. Yu, Q. Dong, and D. Xu, "Discrete-time repetitive control-based ADRC for current loop disturbances suppression of PMSM drives," *IEEE Transactions on Industrial Informatics*, vol. 18, no. 5, pp. 3138–3149, 2022, doi: 10.1109/TII.2021.3107635.
- [16] T. Sreekumar and K. S. Jiji, "Comparison of proportional-integral (P-I) and integral-proportional (I-P) controllers for speed control in vector controlled induction motor drive," in *ICPCES 2012 - 2012 2nd International Conference on Power, Control and Embedded Systems*, 2012, doi: 10.1109/ICPCES.2012.6508089.
- [17] S. H. Samudera, M. M. H. Rifadil, I. Ferdiansyah, S. D. Nugraha, O. A. Qudsi, and E. Purwanto, "Three phase induction motor dynamic speed regulation using IP controller," in *2020 3rd International Seminar on Research of Information Technology and Intelligent Systems, ISRITI 2020*, 2020, pp. 406–411, doi: 10.1109/ISRITI51436.2020.9315340.
- [18] F. Mendoza-Mondragon, V. M. Hernandez-Guzman, and J. Rodriguez-Resendiz, "Robust speed control of permanent magnet synchronous motors using two-degrees-of-freedom control," *IEEE Transactions on Industrial Electronics*, vol. 65, no. 8, pp. 6099–6108, 2018, doi: 10.1109/TIE.2017.2786203.
- [19] P. Chen and Y. Luo, "A two-degree-of-freedom controller design satisfying separation principle with fractional-order PD and generalized ESO," *IEEE/ASME Transactions on Mechatronics*, vol. 27, no. 1, pp. 137–148, 2022, doi: 10.1109/TMECH.2021.3059160.
- [20] S.-H. Kim, "Control of direct current motors," in *Electric Motor Control*, Elsevier, 2017, pp. 39–93, doi: 10.1016/B978-0-12-812138-2.00002-7.





- [21] Z. Lyu and L. Wu, "Current control scheme for LC-equipped PMSM drive considering decoupling and resonance suppression in synchronous complex-vector frame," *IEEE Journal of Emerging and Selected Topics in Power Electronics*, vol. 11, no. 2, pp. 2061–2073, 2023, doi: 10.1109/JESTPE.2022.3218906.
- [22] H. Kim, M. W. Degner, J. M. Guerrero, F. Briz, and R. D. Lorenz, "Discrete-time current regulator design for AC machine drives," *IEEE Transactions on Industry Applications*, vol. 46, no. 4, pp. 1425–1435, 2010, doi: 10.1109/TIA.2010.2049628.
- [23] R. Errouissi, A. Al-Durra, and S. M. Muyeen, "Experimental validation of a novel PI Speed controller for AC motor drives with improved transient performances," *IEEE Transactions on Control Systems Technology*, vol. 26, no. 4, pp. 1414–1421, 2018, doi: 10.1109/TCST.2017.2707404.
- [24] A. M. Diab *et al.*, "Fast and simple tuning rules of synchronous reference frame proportional-integral current controller," *IEEE Access*, vol. 9, pp. 22156–22170, 2021, doi: 10.1109/ACCESS.2021.3054845.
- [25] J. W. Choi and S. C. Lee, "Antiwindup strategy for PI-type speed controller," *IEEE Transactions on Industrial Electronics*, vol. 56, no. 6, pp. 2039–2046, 2009, doi: 10.1109/TIE.2009.2016514.

BIOGRAPHIES OF AUTHORS







Panuwat Kaewma     received the B.Eng. degree in electrical engineering from University of Phayao, Thailand, in 2022. He is currently studying toward M.Eng. degree in electrical engineering from University of Phayao. His research interests include the areas of electric motor drives and flux-weakening control strategies. He can be contacted at email: 65103498@up.ac.th.



Nattapong Pothi     received the B.Eng. and M.Eng. degrees both in electrical engineering from Chiang Mai university, Thailand, in 2003 and 2007, respectively, and Ph.D. degree in electronic and electrical engineering from University of Sheffield, Sheffield, U.K., in 2016. Since 2007, he has been with the school of Engineering, University of Phayao, Thailand, where he is currently an assistant professor in the Department of Electrical Engineering, University of Phayao. His research interests include the areas of electric motor drives, flux-weakening control strategies, energy conversion systems, and power electronic applications. He can be contacted at email: nattapong.po@up.ac.th.



Chawasak Rakpenthai     received the B.Eng., M.Eng., and Ph.D. degrees in electrical engineering from Chiang Mai University, Thailand, in 1999, 2003, and 2007, respectively. He is currently an associate professor at the Department of Electrical Engineering, University of Phayao. His research interests include applications of artificial intelligence in power system, power electronics, power system state estimation, and FACTS devices. He can be contacted at email: chawasak.ra@up.ac.th.